2025 IEEE 19th International Conference on Control & Automation (ICCA)
June 30 - July 3, 2025. Tallinn, Estonia

Fixed-Relative-Switched Threshold Strategies for Consensus Tracking Control of Nonlinear Multiagent Systems

Ziming Wang[1], Yun Gao[1], Apostolos I. Rikos[2], Ning Pang[3], and Yiding Ji[1*]

***Abstract*— This paper investigates event-triggered consensus tracking in nonlinear semi-strict-feedback multi-agent systems (MASs) involving one leader and multiple followers. We first employ radial basis function neural networks (RBFNNs) and backstepping techniques to approximate the unknown nonlinear dynamics, facilitating the design of dual observers to measure the unknown states and disturbances. Then three adaptive event-triggered control (ETC) schemes are proposed: fixed-threshold, relative-threshold, and switched-threshold configurations, each featuring specialized controller architectures and triggering mechanisms. Through Lyapunov stability analysis, we establish that the follower agents can asymptotically track the reference trajectory of the leader, meanwhile, all error signals remain uniform bounded. Our proposed control strategies effectively prevent Zeno behaviors through stringent exclusion criteria. Finally, an empirical case study is presented, which demonstrates the competitive performance of our control framework in terms of achieving consensus tracking and optimizing the triggering efficiency.**

***Index Terms*— Multiagent systems, consensus tracking, observer design, event-triggered control, learning-based control**

I. Introduction

For decades, both control and learning communities have extensively investigted consensus tracking of nonlinear MASs due to its wide applications such as power grids [1], [2], intelligent transportation [3]–[5] and communication systems [6], [7]. The primary objective is to ensure that all units in the network operate ”unanimously” along a desired trajectory and achieve consensus [8], [9]. However, the presence of uncertain system parameters and external perturbations in real engineering scenarios poses considerable challenges for consensus tracking, often rendering existing methods fail to work. Consequently, developing strategies that efficiently tackle the issues is vital.

In the conventional settings of the sample-data control system, controllers continuously respond to changes in the system, which often results in unnecessary resource usage, particularly when the network has restricted bandwidth. A pivotal study [12] highlighted the benefits of ETC compared to periodic impulse control in stochastic systems with noise, resulting in its extensive use in both linear and nonlinear systems. Recent advancements in controller design such as [10]–[20] have further propelled the field of ETC.

The application of ETC to nonlinear systems has achieved notable success in reducing trigger frequency and enhancing control performance [10], [11]. This framework has since been extended by introducing new triggering conditions. For instance, [10] proposed a dynamic triggering condition that alleviates the traditional periodic execution requirements in closed-loop nonlinear systems. The work in [11] utilized the current state of the plant to determine triggering time instances without the requirement of periodicity. More recently, event-triggered mechanisms have been extensively explored within the context of MASs. Notably, [13] introduced a capped-threshold ETC strategy which aims to achieve robust consensus tracking in continuous nonlinear MASs amidst attacks, and [15] employed a switching-based trigger strategy for consensus tracking. Additionally, [18] analyzed three ETC strategies in nonlinear uncertain systems, which did not require input-to-state stability.

In light of these results, we propose an adaptive consensus tracking framework for high-order MASs, which integrates the backstepping method, filtering techniques, RBF NNs, and observers. Our key contributions are summarized as follows:

- We employ RBF NNs with backstepping method to approximate the unknown transition functions of the MASs;
- We develop observers to monitor both unknown states and unmeasured disturbances, which later enhance the robustness of the controller against perturbations;
- We propose three ETC strategies: fixed-threshold, relative-threshold, and switched-threshold, then highlight their performance in terms of reduced control update frequency, improved resource utilization, and extended controller lifespan in the empirical study.

The rest of the paper is structured as follows. Section II reviews preliminary knowledge of MAS, observer design and graph theory, then formulates the key problem of the work. Section III develops the fixed-relative-switched threshold control strategies and analyzes the stability of the strategies. Section IV presents simulation to validate the performance of our method. Finally, Section V summarizes the work and lists several future research directions.

[1]Z. Wang, Y. Gao, and Y. Ji are with Robotics and Autonomous Systems Thrust, The Hong Kong University of Science and Technology (Guangzhou), Guangzhou, China. (E-mails: zwang216@connect.hkust-gz.edu.cn, y.gao@gaoyunailab.com, jiyiding@hkust-gz.edu.cn).

[2]A. I. Rikos is with the Artificial Intelligence Thrust, The Hong Kong University of Science and Technology (Guangzhou), Guangzhou, China. (Email: apostolosr@hkust-gz.edu.cn)

[3]N. Pang is with the Department of Automation, Shanghai Jiao Tong University, Shanghai, China. (Email: ningpangswu76@163.com)

This work is supported by National Natural Science Foundation of China grants 62303389 and 62373289; Guangdong Basic and Applied Research Funding grants 2022A151511076 and 2024A1515012586; Guangdong Research Platform and Project Scheme grant 2024KTSCX039; Guangzhou Basic and Applied Basic Research Scheme grant 2023A04J1067; Guangzhou-HKUST(GZ) Joint Funding grants 2023A03J0678, 2023A03J0011, 2024A03J0618, 2024A03J0680 and 2025A03J3960.

II. Preliminaries and Problem Formulation

A. MAS Model

Imagine a group with a leader labeled 0 and N followers labeled from 1 to N., they communicate with each other in a directed graph and form the MAS model [23] [24]:

$$\begin{aligned} \dot{x}_{i,r} &= x_{i,r+1} + f_{i,r}(\bar{x}_{i,r}) + \xi_{i,r} \\ \dot{x}_{i,n} &= u_i + f_{i,n}(\bar{x}_{i,n}) + \xi_{i,n} \\ y_i &= x_{i,1} \end{aligned} \tag{1}$$

where $i = 1, ..., N$, $j = 1, ..., n$, $r = 1, ..., n-1$, $\bar{x}_{i,j} = [x_{i,1}, ..., x_{i,j}]^T$ are the state of the ith follower, while $u_i \in R$ denotes its input of control. The output of the ith follower is expressed as $y_i \in R$. The function $f_{i,j}(\bar{x}_{i,j})$ represents C^1 class nonlinear smooth equation vectors. $\xi_{i,j}$ represents unmeasured external perturbations affecting the system. Notably, the leader's movement occurs independently without being influenced by the actions or positions of the followers.

B. Observer Design

To effectively locate the unknown states and perturbations throughout the entire control system, we introduce a series of observers. By precisely analyzing and processing feedback data, these observers accurately identify and estimate unknown variables within the system, enhancing the overall robustness and stability. The state observer is defined as

$$\begin{aligned} \dot{\hat{\bar{x}}}_{i,n} &= (P_i \otimes I_m)\dot{\hat{\bar{x}}}_{i,n} + (Q_i \otimes y_i) + \sum_{l=1}^{n}(R_{i,l} \otimes \hat{f}_{i,l}(\dot{\hat{\bar{x}}}_{i,l})) \\ &\quad + (U_i \otimes u_i) + \hat{\varpi}_i \\ y_i &= (V_i^T \otimes I_m)\hat{\bar{x}}_n \end{aligned} \tag{2}$$

where $\otimes$ represents the Kronecker product, and $\hat{\bar{x}}_{i,l} = [\hat{x}_{i,1}^T, \ldots, \hat{x}_{i,l}^T]^T$ represents the estimated value of the actual state with $l = 1, ..., n$. The vector $Q_i = [q_{i,1}, ..., q_{i,n}]^T$ is such that the matrix P_i is a strictly Hurwitz. The parameters are defined as follows: $R_{i,l} = [0, \ldots, 1, \ldots, 0]_{n\times 1}^T$ where the l-th element is 1, $U_i = [0, ..., 0, 1]_{n\times 1}^T$, $V_i = [1, 0, ..., 0]_{n\times 1}^T$ and $P_i = [-Q_i, R_{i,1}, \ldots, R_{i,n-1}]$.

We denote by $\psi_i = [(x_{i,1} - \hat{x}_{i,1})^T, ..., (x_{i,n} - \hat{x}_{i,n})^T]^T$ the error of state observation and have that

$$\dot{\psi}_i = (P_i \otimes I_m)\psi_i + \widetilde{\varpi}_i + \sum_{l=1}^{n} S_{i,l} \otimes (f_{i,l}(\overline{x}_{i,l}) - \hat{f}_{i,l}(\hat{\bar{x}}_{i,l})) \tag{3}$$

We also denote the error of function approximation by $\varphi_i(t) = \sum_{l=1}^{n} R_{i,l} \otimes (f_{i,l}(\bar{x}_{i,l}) - \hat{f}_{i,l}(\hat{\bar{x}}_{i,l}))$ and write $\varphi_i(t) = \left[\varphi_{i,1}^T(t), ..., \varphi_{i,n}^T(t)\right]^T$. Suppose that $\varphi_i(t)$ is bounded, thus there exists an unspecified parameter $\varphi_i^0 > 0$ such that the inequality $\|\varphi_i(t)\| \le \varphi_i^0$ holds. Using RBF NNs to approximate the unidentified nonlinear function of the MASs (1), an optimal weight vector $W_{i,l}^*$ is derived as:

$$f_{i,l}(\bar{x}_{i,l}) = W_{i,l}^{*T} E_{i,l}\left(\hat{\bar{x}}_{i,l}\right) + \sigma_{i,l}(t) \tag{4}$$

where $\sigma_{i,l}(t)$ represents the bounded approximation error, i.e., there is a parameter $\sigma_{0,l} > 0$ such that $|\sigma_{i,l}(t)| \le \sigma_{0,l}$.

Let $\hat{W}_{i,l}^T$ be the estimation of $W_{i,l}^{*T}$, then the estimated smooth nonlinear function is $\hat{f}_{i,l} = \hat{W}_{i,l}^T E_{i,l}$. The optimal weight $W_{i,l}^*$ for $l = 1, \ldots, n$ is designed as:

$$W_{i,l}^* = \arg \min_{\hat{W}_{i,l} \in \breve{\Omega}} \sup_{\substack{\bar{x}_{i,l} \in \Omega_{i,l} \\ \hat{\bar{x}}_{i,l} \in \hat{\Omega}_{i,l}}} \left| \hat{f}_{i,l} - f \right| \tag{5}$$

where $\Omega_{i,l}$, $\hat{\Omega}_{i,l}$ and $\breve{\Omega}$ represent compact sets corresponding to $\bar{x}_{i,l}$, $\hat{\bar{x}}_{i,l}$, $\hat{E}_{i,l}$.

The state observers is then revised as: $\forall 1 \le r < n$

$$\begin{aligned} \dot{\hat{x}}_{i,r} &= \hat{x}_{i,r+1} + \hat{W}_{i,r}^T E_{i,r}\left(\hat{\bar{x}}_{i,r}\right) + q_{i,r}\psi_{i,1} + \hat{\varpi}_{i,r} \\ \dot{\hat{x}}_{i,n} &= u_i + \hat{W}_{i,n}^T E_{i,n}\left(\hat{\bar{x}}_{i,n}\right) + q_{i,n}\psi_{i,1} + \hat{\varpi}_{i,n} \end{aligned} \tag{6}$$

Next, we define the estimate of unknown external perturbations as $\hat{\varpi}_i = [\hat{\varpi}_{i,1}^T, ..., \hat{\varpi}_{i,n}^T]^T$. To facilitate consensus control, we incorporate an auxiliary variable $\tau_{i,l} = \varpi_{i,l} - \kappa_{i,l}x_{i,l}$,where $\kappa_{i,l}$ is a designed positive parameter.

Given the above concepts, the perturbation observer is:

$$\begin{aligned} \hat{\varpi}_{i,l} &= \hat{\tau}_{i,l} + \kappa_{i,l}\hat{x}_{i,l} \\ \dot{\hat{\tau}}_{i,l} &= -\kappa_{i,l}(\hat{W}_{i,l}^T E_{i,l}(\hat{\bar{x}}_{i,l}) + \hat{\tau}_{i,l} + \kappa_{i,l}\hat{x}_{i,l} + \hat{x}_{i,l+1}) \end{aligned} \tag{7}$$

where $x_{i,n+1} = u_i$ and $\hat{W}_{i,l}$ is the estimation of $W_{i,l}^*$.

C. Directed Graph

Given MASs with N followers and a single leader, the interactions among agents are represented by a directed graph $\mathcal{G} = (\mathcal{V}, \mathcal{E})$, where $\mathcal{V} = \{1, ..., N\}$ represents the set of nodes, $\mathcal{E} \subseteq \mathcal{V} \times \mathcal{V}$ represents the edges, and $(\mathcal{V}_i, \mathcal{V}_j) \in \mathcal{E}$ indicates that agent j can receive information from agent i. The matrix $\mathcal{A} = [a_{i,j}]$ of $\mathcal{G}$ is specified as:

$$a_{i,j} = \begin{cases} 0, & if\ (\mathcal{V}_i, \mathcal{V}_j) \notin \mathcal{E} \\ 1, & if\ (\mathcal{V}_i, \mathcal{V}_j) \in \mathcal{E} \end{cases} \tag{8}$$

We define the Laplacian matrix $\mathcal{L}$ as $\mathcal{L} = \mathcal{D} - \mathcal{A}$, where $\mathcal{D} = diag(d_1, ..., d_N)$ is the in-degree matrix of graph $\mathcal{G}$, $d_i = \sum_{j=1, j\neq i}^{N} a_{ij}$. To elucidate, the diagonal matrix $\mathcal{B} = diag\left(\mathcal{C}_1, ..., \mathcal{C}_N\right)$ is defined such that if the leader can relay information to agent i, then the condition $\mathcal{C}_i > 0$. If not, $\mathcal{C}_i = 0$ holds.

D. Problem Formulation

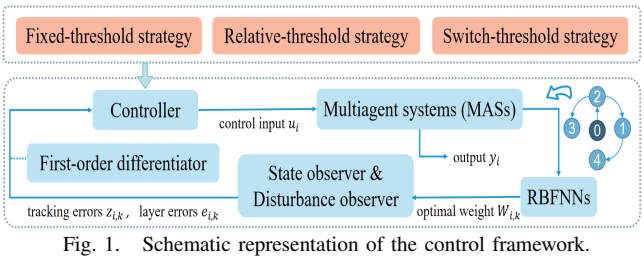

Fig. 1. Schematic representation of the control framework.

Fig. 1 illustrates our framework of adaptive event-triggered consensus tracking control. The following lemmas and assumptions are necessary to facilitate the later discussions.

Lemma 1 (from [21]). *For any positive definite matrix $H_i = H_i^T > 0$, with a symmetric positive matrix F_i and a strict Hurwitz matrix P_i, it satisfies $P_i^T F_i + F_i P_i = -2H_i$.*

Lemma 2 (from [22]). *Inequality $0 \leq |\chi| - \chi \tanh(\frac{\chi}{\chi_0}) \leq 0.2785\chi_0$ holds for any parameter $\chi \in R$ and $\chi_0 > 0$.*

Assumption 1 (from [15], [23], [26]). *The unmeasured external perturbations are all bounded, i.e., inequality $\|\varpi_{i,j}\| \leq \varpi_{i,j}^0$ holds, where $\varpi_{i,j}^0$ is a positive parameter.*

Assumption 2 (from [24]). *In the MAS, the leader's target reference signal is not only smooth but also measurable, with both $y_r(t)$ and $\dot{y}_r(t)$ being bounded.*

Problem 1 (Consensus tracking of MASs). *Given a class of nonlinear MASs following equation (1), suppose that the communication of agents is modeled by a directed graph $\mathcal{G}$, each follower is subject to unknown external perturbations ξ and required to track the leader's reference signal y_r, then our goals are two-fold: (i) design an adaptive control law to ensure that the tracking errors are uniformly bounded; (ii) evaluate the performance of different event-triggered threshold control strategies in terms of control update frequency, resources conservation and controller's lifespan.*

III. Event-Triggered Controller Design

This section is initiated by the general procedure of controller design for Problem 1. First, the graph-based errors $z_{i,r}$ and boundary layer errors $e_{i,r}$ for the i-th follower are:

$$\begin{aligned} z_{i,1} &= \sum_{j=1}^{N} a_{i,j}(y_i - y_j) + b_i(y_i - y_r) \\ z_{i,r} &= x_{i,r} - \bar{\alpha}_{i,r} \\ e_{i,r} &= \bar{\alpha}_{i,r} - \alpha_{i,r} \end{aligned} \tag{9}$$

where $r = 2, ..., n$. The terms $\alpha_{i,r}$ and $\bar{\alpha}_{i,r}$ respectively denote the virtual control and its filtered counterpart.

Step 1: The Lyapunov function is determined as

$$\begin{aligned} V_{i,1} &= \frac{z_{i,1}^2}{2} + \frac{\tilde{\tau}_{i,1}^2}{2} + \frac{1}{2\eta_{i,1}}\tilde{W}_{i,1}^T\tilde{W}_{i,1} + \frac{1}{2o_i}\tilde{\Theta}_i^2 + V_0 \\ V_0 &= \frac{1}{2}\psi_i^T(F_i \otimes I_m)\psi_i \end{aligned} \tag{10}$$

where $\psi_i = [\psi_{i,1}^T, ..., \psi_{i,n}^T]^T$, $\eta_{i,1} > 0$ and $o_i > 0$ define designed parameters. Then, define an auxiliary function as

$$\begin{aligned} \bar{Z}_{i,1}(T_{i,1}) = &- \sum_{j=1}^{N} a_{i,j}\left(\hat{x}_{j,2} + f_{j,1}(\bar{x}_{j,1}) + \varpi_{j,1} + \psi_{j,2}\right) \\ &+ (d_i + b_i)\left(f_{i,1}(\bar{x}_{i,1}) + \varpi_{i,1} + \psi_{i,2}\right) - b_i\dot{y}_r. \end{aligned} \tag{11}$$

$\bar{Z}_{i,1}$ is approximated by RBF NNs: $\bar{Z}_{i,1} = K_{i,1}^{*T}E_{i,1} + \delta_{i,1}$, where $\bar{\delta}_{i,1}$ defines an unknown positive parameter, $T_{i,1} = [y_r, \dot{y}_r, \hat{x}_{i,1}^T, \hat{x}_{j,1}^T, \hat{\varpi}_{i,1}^T, \hat{\varpi}_{j,1}^T]^T$ denotes the input of RBF NNs and $K_{i,1}^{*T}$ is the optimal weight, just like the $W_{i,1}^{*T}$ in (4)(5), with $|\delta_{i,1}(T_{i,1})| \leq \bar{\delta}_{i,1}$.

Utilizing Young's inequality, with a positive designed parameter $c_{i,1}$, the subsequent inequality can be derived:

$$z_{i,1}\bar{Z}_{i,1} \leq \frac{\Theta_i^*}{2c_{i,1}^2}z_{i,1}^2E_{i,1}^TE_{i,1} + \frac{c_{i,1}^2}{2} + \frac{z_{i,1}^2}{2} + \frac{\bar{\delta}_{i,1}^2}{2} \tag{12}$$

By Young's inequality and Assumption 1, one has

$$\psi_i^T(F_i \otimes I_m)\varphi_i \leq \frac{1}{2}\|F_i \otimes I_m\|^2\left\|\varphi_i^0\right\|^2 + \frac{1}{2}\|\psi_i\|^2 \tag{13}$$

$$\psi_i^T(F_i \otimes I_m)\tilde{\varpi}_i \leq \frac{1}{2}\|F_i \otimes I_m\|^2\left\|\tilde{\varpi}_i^0\right\|^2 + \frac{1}{2}\|\psi_i\|^2 \tag{14}$$

The virtual and adaptive control laws are formulated as

$$\alpha_{i,2} = \frac{1}{d_i + b_i}(r_{i,1}z_{i,1} - \frac{z_{i,1}}{2} - \frac{\hat{\Theta}_i}{2c_{i,1}^2}z_{i,1}E_{i,1}^TE_{i,1}) \tag{15}$$

$$\dot{\hat{W}}_{i,1} = -h_{i,1}\hat{W}_{i,1} - \eta_{i,1}\tilde{\tau}_{i,1}\kappa_{i,1}E_{i,1}\left(\hat{\bar{x}}_{i,1}\right) \tag{16}$$

where $h_{i,1}$ and $r_{i,1}$ are designed parameters. Then, considering Lemma 1 and the above formulas, one has

$$\begin{aligned} \dot{V}_{i,1} \leq &r_{i,1}z_{i,1}^2 + (d_i + b_i)z_{i,1}(z_{i,2} + e_{i,2}) + \tilde{\tau}_{i,1}\dot{\varpi}_{i,1} \\ &+ (\frac{3 - 2\kappa_{i,1}}{2})\tilde{\tau}_{i,1}^2 + \iota_{i,1} + \frac{h_{i,1}}{\eta_{i,1}}\tilde{W}_{i,1}^T\hat{W}_{i,1} \\ &+ \tilde{\Theta}_i(\frac{1}{2c_{i,1}^2}z_{i,1}^2E_{i,1}^TE_{i,1} - \frac{\dot{\hat{\Theta}}_i}{o_i}) \\ &- \psi_i^T(H_i \otimes I_m)\psi_i + (1 + \kappa_{i,1}^2 + \kappa_{i,1}^4)\|\psi_i\|^2 \end{aligned} \tag{17}$$

where $\iota_{i,1} = \frac{c_{i,1}^2}{2} + \frac{\bar{\delta}_{i,1}^2}{2} + \frac{\kappa_{i,1}^2\sigma_{0,1}^2}{2} + \frac{1}{2}\left\|\varphi_i^0\right\|^2\|F_i \otimes I_m\|^2 + \frac{1}{2}\left\|\tilde{\varpi}_i^0\right\|^2\|F_i \otimes I_m\|^2$. Then, with a small positive designed parameter $m_{i,2}$, process $\alpha_{i,2}$ through the first-order low-pass filter, resulting in $\bar{\alpha}_{i,2}$ as follows:

$$\begin{aligned} \bar{\alpha}_{i,2}(0) &= \alpha_{i,2}(0) \\ m_{i,2}\dot{\bar{\alpha}}_{i,2} + \bar{\alpha}_{i,2} &= \alpha_{i,2} \end{aligned} \tag{18}$$

Step r: Choose the Lyapunov function as

$$V_{i,r} = \frac{z_{i,r}^2}{2} + \frac{\tilde{\tau}_{i,r}^2}{2} + \frac{1}{2\eta_{i,r}}\tilde{W}_{i,r}^T\tilde{W}_{i,r} \tag{19}$$

where $\eta_{i,r} > 0$ is a parameter. By utilizing RBF NNs, one has $\bar{Z}_{i,r} = K_{i,r}^{*T}E_{i,r}(T_{i,r}) + \delta_{i,r}$, where $\bar{\delta}_{i,r} > 0$ is an unknown parameter, with $|\delta_{i,r}(T_{i,r})| \leq \bar{\delta}_{i,r}$, the control strategy and adaptive parameters are formulated as follows:

$$\begin{aligned} \alpha_{i,r+1} = &r_{i,r}z_{i,r} - \frac{z_{i,r}}{2} + \frac{\alpha_{i,r} - \bar{\alpha}_{i,r}}{m_{i,r}} - q_{i,r}\psi_{i,1} \\ &- \frac{\hat{\Theta}_i}{2c_{i,r}^2}z_{i,r}E_{i,r}^TE_{i,r} \end{aligned} \tag{20}$$

$$\dot{\hat{W}}_{i,r} = -h_{i,r}\hat{W}_{i,r} - \eta_{i,r}\tilde{\tau}_{i,r}\kappa_{i,r}E_{i,r}\left(\hat{\bar{x}}_{i,r}\right) \tag{21}$$

where $T_{i,r} = [y_r, \hat{\Theta}_i, \hat{\bar{x}}_{i,r}^T, \hat{\bar{x}}_{j,r}^T, \hat{\varpi}_{i,r}^T, \hat{\varpi}_{j,r}^T]^T$, $r_{i,r}$ and $h_{i,r}$ are designed parameters. By the Young's inequality, one gets

$$\begin{aligned} \dot{V}_{i,r} \leq &r_{i,r}z_{i,r}^2 + \left(\kappa_{i,r}^2 + \kappa_{i,r}^4\right)\|\psi_i\|^2 + z_{i,r}(z_{i,r+1} + e_{i,r+1}) \\ &+ \frac{h_{i,r}}{\eta_{i,r}}\tilde{W}_{i,r}^T\hat{W}_{i,r} + (\frac{3 - 2\kappa_{i,r}}{2})\tilde{\tau}_{i,r}^2 + \tilde{\tau}_{i,r}\dot{\varpi}_{i,r} \\ &+ \frac{\tilde{\Theta}_i}{2c_{i,r}^2}z_{i,r}^2E_{i,r}^TE_{i,r} + \iota_{i,r} \end{aligned} \tag{22}$$

where $\iota_{i,r} = \frac{c_{i,r}^2}{2} + \frac{\bar{\delta}_{i,r}^2}{2} + \frac{\kappa_{i,r}^2 \sigma_{0,r}^2}{2}$ and $c_{i,r}0 > 0$. In line with Step 1, the filter is implemented as:

$$\begin{aligned} &\bar{\alpha}_{i,r+1}(0) = \alpha_{i,r+1}(0) \\ &m_{i,r+1}\dot{\bar{\alpha}}_{i,r+1} + \bar{\alpha}_{i,r+1} = \alpha_{i,r+1} \end{aligned} \tag{23}$$

where $m_{i,r+1}$ denotes a slight positive designed parameter.

Step n: Define the Lyapunov function as

$$V_{i,n} = \frac{z_{i,n}^2}{2} + \frac{\tilde{\tau}_{i,n}^2}{2} + \frac{1}{2\eta_{i,n}} \tilde{W}_{i,n}^T \tilde{W}_{i,n} \tag{24}$$

where $\eta_{i,n}$ denotes a designed positive parameter. By RBF NNs, one has $\bar{Z}_{i,n} = K_{i,n}^{*T} E_{i,n} + \delta_{i,n}$, where $\bar{\delta}_{i,n}$ denotes an unknown positive parameter, with $|\delta_{i,n}(T_{i,n})| \leq \bar{\delta}_{i,n}$. With designed parameters $r_{i,n}$, $h_{i,n}$, λ_i, the control strategy and adaptive parameters are formulated as follows:

$$\begin{aligned} \alpha_{i,n+1} =& r_{i,n} z_{i,n} - \frac{z_{i,n}}{2} + \frac{\alpha_{i,n} - \bar{\alpha}_{i,n}}{m_{i,n}} - q_{i,n}\psi_{i,1} \\ &- \frac{\hat{\Theta}_i}{2c_{i,n}^2} z_{i,n} E_{i,n}^T E_{i,n} \end{aligned} \tag{25}$$

$$\dot{\hat{W}}_{i,n} = -h_{i,n}\hat{W}_{i,n} - \eta_{i,n}\tilde{\tau}_{i,n}\kappa_{i,n} E_{i,n}\left(\hat{\bar{x}}_{i,n}\right) \tag{26}$$

$$\dot{\hat{\Theta}}_i = -\lambda_i \hat{\Theta}_i + \sum_{k=1}^{n} \frac{o_i}{2c_{i,k}^2} z_{i,k}^2 E_{i,k}^T E_{i,k} \tag{27}$$

We now develop three ETC strategies that provably ensure consensus tracking for the MASs. Theoretical analysis is also provided for their convergence.

A. Fixed-threshold strategy

The ETC controller is reformulated as

$$w_i(t) = \alpha_{i,n+1} - \bar{\pi}_i \tanh\left(\frac{z_{i,n}\bar{\pi}_i}{\mu_i}\right) \tag{28}$$

where the triggering condition is designed as

$$u_i(t) = w_i(t_s) \ , \ \forall \mathrm{t} \in [t_s, t_{s+1}) \tag{29}$$

$$t_{s+1} = \inf\{\mathrm{t} \in R || \vartheta_i(t)| \geq \pi_i\}, \mathrm{t}_1 = 0 \tag{30}$$

where $\vartheta_i(t) = w_i(t) - u_i(t)$ is the controller error and t_s is the controller's triggering time with $s \in Z$. The parameters $\bar{\pi}_i$, π_i and μ_i are designed to be positive with $\bar{\pi} > \pi_i$. The control signal $u_i(t_{s+1})$ is applied to the system when condition (30) is activated. During the interval $\mathrm{t} \in [t_s, t_{s+1})$, i.e. $|w_i(t) - u_i(t)| < \pi_i$, the controller maintains a constant value of $w_i(t_s)$. For a function $\epsilon_i(t)$ that continuously changes over time and satisfies $\epsilon_i(t_s) = 0$ and $\epsilon_i(t_{s+1}) = \pm 1$ with $|\epsilon_i(t)| \leq 1$, it follows that $w_i(t) = u_i(t) + \epsilon_i(t)\pi_i$. By Lemma 2, $-\epsilon_i(t)\pi_i z_{i,n} - \bar{\pi}_i z_{i,n} \tanh(\frac{z_{i,n}\bar{\pi}_i}{\mu_i}) \leq 0.2875\mu_i$ holds, then we differentiate $V_{i,n}$ by the Young's inequality and (25)-(27), with $\iota_{i,n} = \frac{c_{i,n}^2}{2} + \frac{\bar{\delta}_{i,n}^2}{2} + \frac{\kappa_{i,n}^2\sigma_{0,n}^2}{2} + 0.2785\mu_i$ and a positive parameter $c_{i,n}$, and get the result below:

$$\begin{aligned} \dot{V}_{i,n} \leq& r_{i,n} z_{i,n}^2 + \left(\frac{3 - 2\kappa_{i,n}}{2}\right)\tilde{\tau}_{i,n}^2 + \tilde{\tau}_{i,n}\dot{\varpi}_{i,n} \\ &+ \frac{\tilde{\Theta}_i}{2c_{i,n}^2} z_{i,n}^2 E_{i,n}^T E_{i,n} + \iota_{i,n} \\ &+ \frac{h_{i,n}}{\eta_{i,n}} \tilde{W}_{i,n}^T \hat{W}_{i,n} + \left(\kappa_{i,n}^2 + \kappa_{i,n}^4\right)\|\psi_i\|^2 \end{aligned} \tag{31}$$

B. Relative-threshold strategy

Within the fixed-threshold strategy, the threshold π_i is a constant value, irrespective of the control signal's intensity. However, it is preferable to set a variable threshold for the triggering condition to achieve system stabilization [25]. Notably, when the control signal u_i is huge, a greater error is tolerated, allowing for longer update intervals. Conversely, when u_i approaches 0, the system states stabilize towards equilibrium and a smaller threshold enables more accurate control, improving the overall performance. Then, we propose the ETC controller:

$$\begin{aligned} w_i(t) =& -(1 + \Delta_i)(\alpha_{i,n+1} tanh(\frac{z_{i,n}\alpha_{i,n+1}}{\mu_i}) \\ &+ \bar{\pi}_i^* \tanh(\frac{z_{i,n}\bar{\pi}_i^*}{\mu_i})) \end{aligned} \tag{32}$$

The triggering condition is designed as

$$u_i(t) = w_i(t_s) \ , \ \forall \mathrm{t} \in [t_s, t_{s+1}) \tag{33}$$

$$t_{s+1} = \inf\{\mathrm{t} \in R || \vartheta_i(t)| \geq \Delta_i |u_i(t)| + \pi_i^*\} \tag{34}$$

where t_s represents the time when the controller is updated, $s \in Z$, μ_i, Δ_i, $0 < \Delta_i < 1$, $\pi_i^* > 0$, and $\bar{\pi}_i^* > \pi_i^*/(1 - \Delta_i)$ are all positive designed parameters. From (34), we have $w_i(t) = (1 + \rho_{1,i}(t))u_i(t) + \rho_{2,i}(t)\pi_i^*$ in the interval $[t_s, t_{s+1}]$, where $\rho_{1,i}(t)$ and $\rho_{2,i}(t)$ denote time-varying parameters satisfying $|\rho_{1,i}(t)| \leq 1$ and $|\rho_{2,i}(t)| \leq 1$. Thus, one has

$$u_i(t) = \frac{w_i(t)}{1 + \rho_{1,i}(t)\Delta_i} - \frac{\rho_{2,i}(t)\pi_i^*}{1 + \rho_{1,i}(t)\Delta_i} \tag{35}$$

According to the above analysis, similar to (31), it can be obtained the same derivative result of $\dot{V}_{i,n}$ with different $\iota_{i,n}$, where $\iota_{i,n} = \frac{c_{i,n}^2}{2} + \frac{\bar{\delta}_{i,n}^2}{2} + \frac{\kappa_{i,n}^2\sigma_{0,n}^2}{2} + 0.557\mu_i$.

C. Switched-threshold strategy

We now introduce a switched-threshold strategy. The relative-threshold approach adjusts the threshold based on the control signal's magnitude, allowing for longer update intervals when the signal is huge and more precise control as the signal nears zero, thus improving performance. However, a very large control signal can lead to significant measurement errors and abrupt changes during updates. In contrast, the fixed-threshold strategy maintains a consistent upper limit on measurement errors, regardless of signal size. Then we propose the control strategy whose switching gate G and the triggering condition are designed below:

$$u_i(t) = w_i(t_s) \ , \ \forall \mathrm{t} \in [t_s, t_{s+1}) \tag{36}$$

$$t_{s+1} = \begin{cases} \inf\{\mathrm{t} \in R || \vartheta_i(t)| \geq \Delta_i |u_i(t)| + \pi_i^*\}, |u_i| \geq G \\ \inf\{\mathrm{t} \in R || \vartheta_i(t)| \geq \pi_i\}, |u_i| < G \end{cases} \tag{37}$$

With $t \in [t_s, t_{s+1})$, we get

$$\bar{\vartheta}_i = sup|\vartheta_i(t)| \leq max\{(\Delta_i |u_i(t)| + \pi_i^*), \pi_i\} \tag{38}$$

Since the switched-threshold strategy employs an identical control law for both the fixed-threshold and relative-threshold strategies, the ultimate bounds for tracking and stabilization errors remain consistent with those of the above two.

In summary, we have established an adaptive consensus tracking control framework which integrates state-disturbance observer design, learning based dynamics approximation, backstepping method and three ETC strategies. Finally, we prove that all error signals are bounded by employing Lyapunov stability theory. In addition, we also confirm the soundness of the proposed control strategies that effectively avoid Zeno behaviors.

Theorem 1. *For the MASs in equation (1) under the event-triggered controllers in equation (28)(32), if the initial condition satisfies $V(0) \leq \Omega$, the error signals $z_{i,r}$, $\tilde{c}_{i,r}$, $\tilde{W}_{i,r}$, $\tilde{\Theta}_i$, $e_{i,r}$, and $\psi_{i,r}$ are all uniformly bounded. Furthermore, the consensus tracking errors between the outputs of the followers and the leader's trajectory can be constrained within a predefined range.*

Proof. With $i = 1, ..., N$, define the overall Lyapunov function of the MASs (1) as

$$V = \sum_{i=1}^{N}\sum_{r=1}^{n} V_{i,r} + \sum_{i=1}^{N}\sum_{r=1}^{n-1} \frac{e_{i,r+1}^2}{2} \tag{39}$$

Define the parameters $r_{i,1}$, $r_{i,2}$, $r_{i,r}$ and $r_{i,n}$ as $r_{i,1} = -(d_i + b_i) + r_{i,1}^*$, $r_{i,2} = -\frac{d_i+b_i}{2} - 1 + r_{i,2}^*$, $r_{i,r} = -\frac{3}{2} + r_{i,r}^*$ and $r_{i,n} = -\frac{1}{2} + r_{i,n}^*$ with $r = 3, ..., n-1$. Based on the Young's inequality, while $\|\dot{\varpi}_{i,r}\| \leq \kappa_{i,r}^* \|\tilde{\tau}_{i,r}\|$, one has

$$\begin{aligned}\dot{V} \leq \sum_{i=1}^{N} \Bigg\{ & \sum_{r=1}^{n} r_{i,r}^* z_{i,r}^2 + \sum_{r=2}^{n-1} \frac{e_{i,r+1}^2}{2} + \frac{d_i + b_i}{2} e_{i,2}^2 \\ & + \sum_{r=1}^{n-1} e_{i,r+1}\dot{e}_{i,r+1} + 2\sum_{r=1}^{n} \kappa_{i,r}^* \tilde{\tau}_{i,r}^2 + \frac{\lambda_i}{2o_i}(\Theta_i^{*2} - \tilde{\Theta}_i^2) \\ & + \sum_{r=1}^{n} \frac{h_{i,r}}{2\eta_{i,r}}(W_{i,r}^{*T} W_{i,r}^* - \tilde{W}_{i,r}^T \tilde{W}_{i,r}) + \sum_{r=1}^{n} \iota_{i,r} \\ & - \psi_i^T ((H_i - (1 + \sum_{r=1}^{n} (\kappa_{i,r}^2 + \kappa_{i,r}^4)) I_n) \otimes I_m) \psi_i \Bigg\} \end{aligned} \tag{40}$$

where $\kappa_{i,r}^* = (3 - 2\kappa_{i,r})/2$, $r_{i,r}^*$ and $\kappa_{i,r}^*$ are unknown parameters for stability analysis, with $r = 1, ..., n$. And $\hbar(\bullet)$ is the eigenvalue of the given matrix. Select the matrix H_i such that $\hbar_{\min}[H_i - (1 + \sum_{r=1}^{n} (\kappa_{i,r}^2 + \kappa_{i,r}^4)) I_n] = \wp_i / 2\hbar_{\max}(F_i)$, where $\wp_i$ is a positive parameter. Differentiate $e_{i,2}$ and $e_{i,r+1}$ with respect to time, one has $\dot{e}_{i,2} = -\frac{e_{i,2}}{m_{i,2}} + \Gamma_{i,2}$, $\dot{e}_{i,r+1} = -\frac{e_{i,r+1}}{m_{i,r+1}} + \Gamma_{i,r+1}$, where $\Gamma_{i,2} = -\frac{r_{i,1}\dot{z}_{i,1}}{d_i + b_i} + \frac{\hat{\Theta}_i}{2c_{i,1}^2(d_i+b_i)} \dot{z}_{i,1} E_{i,1}^T E_{i,1} + \frac{\dot{z}_{i,1}}{2(d_i+b_i)} + \frac{\hat{\Theta}_i}{c_{i,1}^2(d_i+b_i)} z_{i,1} E_{i,1}^T \dot{E}_{i,1}$ and $\Gamma_{i,r+1} = \frac{\dot{e}_{i,r}}{m_{i,r}} + q_{i,r}\dot{\psi}_{i,1} + \frac{\hat{\Theta}_i}{2c_{i,r}^2} \dot{z}_{i,r} E_{i,r}^T E_{i,r} - r_{i,r}\dot{z}_{i,r} + \frac{\dot{z}_{i,r}}{2} + \frac{\hat{\Theta}_i}{c_{i,r}^2} z_{i,r} E_{i,r}^T \dot{E}_{i,r}$. Inspired by [24], we have

$$\begin{aligned}\mathbb{M}_{i,r} = \Bigg\{ & \sum_{i=1}^{N}\sum_{r=1}^{n} (z_{i,r}^2 + \tilde{\tau}_{i,r}^2 + \frac{1}{\eta_{i,r}} \tilde{W}_{i,r}^T \tilde{W}_{i,r}) + \sum_{i=1}^{N} \frac{1}{o_i} \tilde{\Theta}_i^2 \\ & + \sum_{i=1}^{N} \psi_i^T (F_i \otimes I_m) \psi_i + \sum_{i=1}^{N}\sum_{r=1}^{n-1} e_{i,r+1}^2 \leq 2\Omega \Bigg\} \end{aligned} \tag{41}$$

where $\mathbb{M}_{i,r}$ is compact in $R^{\dim(\mathbb{C}_{i,r})}$, there exists an inequality $\|\Gamma_{i,r+1}\| \leq L_{i,r+1}$, where $L_{i,r+1}$ denotes a positive parameter. Applying the Young's inequality, one can get $\Gamma_{i,r+1} e_{i,r+1} \leq \frac{\Xi}{2} + \frac{L_{i,r+1}^2 e_{i,r+1}^2}{2\Xi}$, where Ξ is a positive parameter, with $r = 1, ..., n-1$. Select the parameters as $\frac{1}{m_{i,2}} = \frac{d_i + b_i}{2} + \frac{L_{i,2}^2}{2\Xi} + m_{i,2}^*$ and $\frac{1}{m_{i,r+1}} = \frac{1}{2} + \frac{L_{i,r+1}^2}{2\Xi} + m_{i,r+1}^*$, where $m_{i,r+1}^*$ denotes an unknown positive parameter, with $r = 2, ..., n-1$. With $l = 2, ..., n$ and $r = 1, ..., n$, define

$$\beta = \min\left\{-2r_{i,r}^*,\ -4\kappa_{i,r}^*,\ 2m_{i,l}^*,\ h_{i,r},\ \wp_i,\ \lambda_i\right\} \tag{42}$$

$$\gamma = \sum_{i=1}^{N}\sum_{r=1}^{n} (\iota_{i,r} + \frac{h_{i,r}}{2\eta_{i,r}} W_{i,r}^{*T} W_{i,r}^*) + \sum_{i=1}^{N} (\sum_{r=1}^{n-1} \frac{\Xi}{2} + \frac{\lambda_i}{2o_i} (\Theta_i^*)^2) \tag{43}$$

To confirm the stability of the MASs, it is crucial to appropriately select parameter values while adhering to the following conditions: $-r_{i,r}^* > 0$, $-\kappa_{i,r}^* > 0$, $h_{i,r} > 0$, $\wp_i > 0$, $\lambda_i > 0$ and $m_{i,l}^* > 0$. Then, we have

$$\dot{V} \leq -\beta V + \gamma \tag{44}$$

When set $\beta > \gamma/\Delta$, we get $\dot{V} < 0$ on $V = \Delta$. Further, if at time $t = 0$ the condition $V \leq \Delta$ holds, it follows that $V \leq \Delta$ for entire $t > 0$. This demonstrates that the error signals $z_{i,r}$, $e_{i,r}$, $\tilde{\tau}_{i,r}$, $\tilde{W}_{i,r}$, $\tilde{\Theta}_i$ and $\psi_{i,r}$ are uniformly bounded. It is straightforward to derive the following:

$$\frac{1}{2}\|\Upsilon_1\|^2 \leq V(t) \leq e^{-\beta t} V(0) + \frac{\gamma}{\beta}\left(1 - e^{-\beta t}\right) \tag{45}$$

where $\Upsilon = \left[\Upsilon_1^T, \Upsilon_2^T, \ldots, \Upsilon_M^T\right]^T$. Then, we have $\|\Upsilon\|^2 \leq 2e^{-\beta t} V(0) + \frac{2\gamma}{\beta}\left(1 - e^{-\beta t}\right)$.

Consequently, as time progresses, all consensus tracking errors will converge to a compact set defined as $\Im = \{\Upsilon_1 | \, \|\Upsilon_1\| \leq \sqrt{2\gamma/\beta}\}$. This means that the tracking errors can be modified and reduced to an arbitrarily small range by increasing the parameter β. From (30), one has

$$\dot{\alpha}_i(t) = \dot{w}_{i,n+1} - \frac{\bar{\pi}_i \dot{\bar{z}}_{i,n}}{\cosh^2\left(\frac{z_{i,n}\bar{\pi}_i}{\mu_i}\right)} \tag{46}$$

According to [27]–[29], one gets

$$\frac{d}{dt}|\vartheta_i(t)| = sign(\vartheta_i(t))\,\dot{\vartheta}_i(t) \leq |\dot{w}_i(t)| \tag{47}$$

Based on the stability analysis, it is imperative that there exists a positive parameter Π such that $|\dot{w}_i(t)| \leq \Pi$. Based on (29)(30), we have $\vartheta_i(t_s) = 0$ and $\lim_{t \to t_{s+1}} \vartheta_i(t) = \pi_i$. Additionally, for the time interval $t \in [t_s, t_{s+1})$, the lower bound for the inter-execution time is given by $t^* \geq \pi_i/\Pi$. Following the same analysis in the proof of fixed-threshold strategy, according to (33)(34), the relative-threshold and switched-threshold strategy satisfy $t^* \geq (\Delta_i |u_i(t)| + \pi_i^*)/\Pi$ and $t^* \geq max\{\pi_i, \pi_i^*\}/\Pi$, respectively. Consequently, the Zeno behavior is proficiently avoided. □

IV. Illustrative Example

In this section, we provide an simulation to demonstrate the validity and effectiveness of our theoretical approach. The MASs being examined consist of one leader and four followers, with each agent's dynamics characterized by:

$$\begin{aligned}\dot{x}_{i,1} &= x_{i,2} + f_{i,1}\left(\bar{x}_{i,1}\right) + \xi_{i,1}\\ \dot{x}_{i,2} &= u_i + f_{i,2}\left(\bar{x}_{i,2}\right) + \xi_{i,2}\\ y_i(t) &= x_{i,1}\end{aligned} \tag{48}$$

where $f_{i,1}\left(\bar{x}_{i,1}\right) = 0.8x_{i,1}e^{-1.4x_{i,2}^2}$, $f_{i,2}\left(\bar{x}_{i,2}\right) = -0.5x_{i,1}^2\cos\left(x_{i,2}\right)$, $\xi_{i,1} = 0.8x_{i,1}\sin\left(x_{i,2}\right)\cos^2\left(t\right)$ and $\xi_{i,2} = 0.2x_{i,2}\cos\left(x_{i,1}\right)\cos^2\left(t\right)$, $i = 1, ..., 4$. The leader's trajectory signal is defined as $y_r = -0.5\sin(4t)\cos(2t)$.

The communication topology is shown in Fig. 1. The connection matrix linking the leader to the followers is represented as $\mathcal{B} = diag(0, 1, 0, 0)$. And the matrix $\mathcal{A}$ and $\mathcal{L}$ are given as:

$$\mathcal{A} = \begin{bmatrix} 0 & 1 & 0 & 0\\ 0 & 0 & 0 & 0\\ 0 & 1 & 0 & 0\\ 1 & 0 & 0 & 0 \end{bmatrix},\ \mathcal{L} = \begin{bmatrix} 1 & -1 & 0 & 0\\ 0 & 0 & 0 & 0\\ 0 & -1 & 1 & 0\\ -1 & 0 & 0 & 1 \end{bmatrix}$$

The starting conditions for the four followers and their associated state observers are determined as follows:

$\bar{x}_{1,2}(0) = [0.2,\ 0]^T$	$\hat{\bar{x}}_{1,2}(0) = [0.3,\ 1.7]^T$
$\bar{x}_{2,2}(0) = [-0.2,\ 0]^T$	$\hat{\bar{x}}_{2,2}(0) = [-0.5,\ 1.7]^T$
$\bar{x}_{3,2}(0) = [0.1,\ 0]^T$	$\hat{\bar{x}}_{3,2}(0) = [0,\ -4]^T$
$\bar{x}_{4,2}(0) = [-0.3,\ 0]^T$	$\hat{\bar{x}}_{4,2}(0) = [0,\ -4]^T$

The designed parameters are: for fix-threshold strategy, $\pi_i = 2.5$, $\bar{\pi}_i = 4$, $\mu_i = 5.4$, for relative-threshold strategy, $\pi_i^* = 2$, $\bar{\pi}_i^* = 4$, $\Delta_i = 0.245$, for switched-threshold strategy $G = 6$, for the first order low pass filter, $m_i = 0.005$, for other parameters, $h_{i,1} = h_{i,2} = 50$, $r_{i,1} = r_{i,2} = -100$, $c_{i,1} = c_{i,2} = 100$, $\eta_{i,1} = \eta_{i,2} = 0.01$, $q_{i,1} = 350$, $q_{i,2} = 0.5$, $\lambda_i = 120$ and $o_i = 25$.

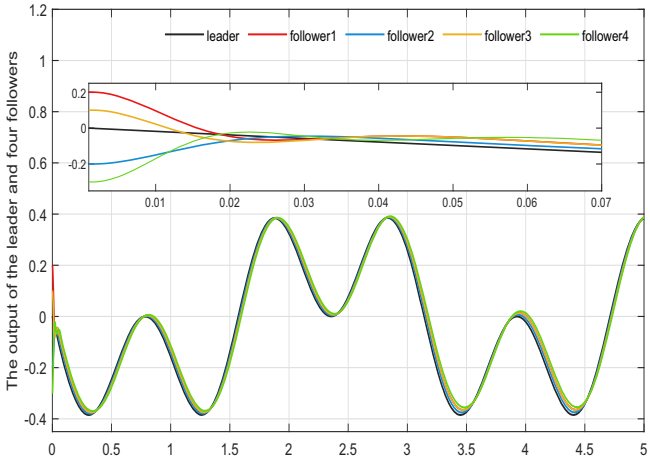

Fig. 2. Consensus tracking performance.

In Fig. 2, shortly after the process begins, all followers within the system consistently follow the leader, successfully

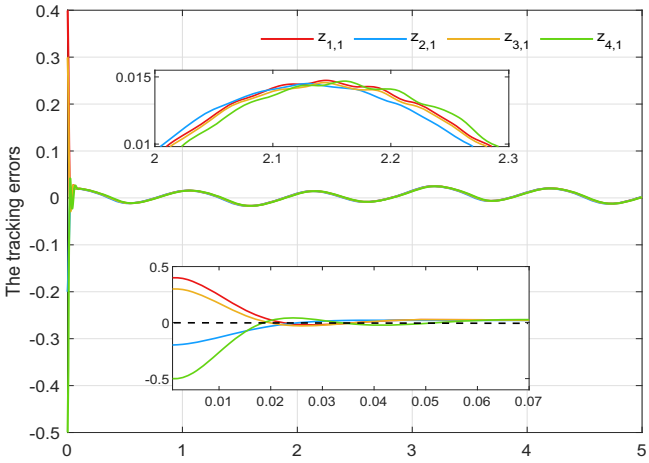

Fig. 3. Trajectories of tracking errors $z_{i,1}(i = 1, 2, 3, 4.)$

achieving adaptive consensus tracking. Fig. 3 demonstrates that the tracking error has reached zero. The total triggering number for the sample-data strategy is 5,000 times, and the triggering numbers for the three threshold strategies are detailed in Table I. Fig. 4 illustrates the range of events activated by each of the three strategies. The data reveal that the fixed-threshold strategy results in the greatest number of activations. Conversely, the relative-threshold strategy produces the fewest activations, whereas the switched-threshold strategy falls in between, the number of triggers falls and both types play an indispensable role in this strategy.

TABLE I
Comparison of three event-triggered strategies.

	Fixed-threshold	Switch-threshold	Relative-threshold
Follower 1	364	$344(255 + 89)$	310
Follower 2	296	$281(220 + 61)$	277
Follower 3	358	$342(255 + 87)$	308
Follower 4	453	$420(306 + 114)$	380

V. Conclusion

This study introduces an observer-based control framework to tackle the consensus tracking issue in nonlinear MASs. RBF NNs are utilized to model the unidentified dynamics, which is then leveraged to build observers to measure unidentified system states and external perturbations. Then we present three ETC strategies and analyze their stability using Lyapunov methods. Our approach successfully mitigates complexity issues through the integration of a filtering mechanism at each design stage. Simulation results demonstrate that the fixed-threshold strategy enhances system performance and minimizes the number of triggering instances. Meanwhile, the relative-threshold strategy further optimizes resource conservation. The switched-threshold strategy achieves a commendable balance between performance improvement and resource utilization. In our forthcoming research, we intend to broaden the existing framework to tackle optimal control issues associated with stochastic nonlinear MASs.

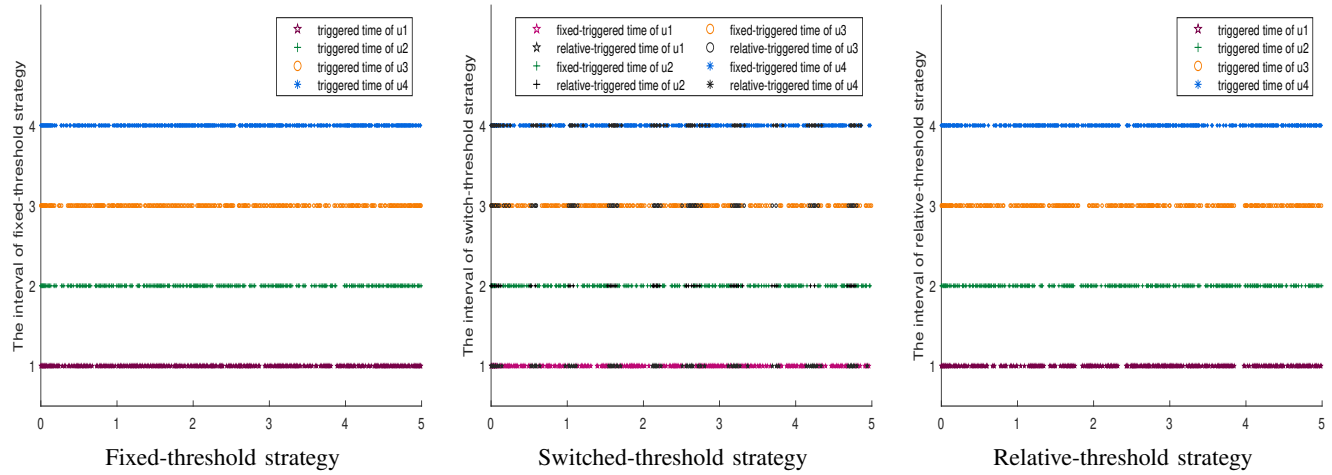

Fig. 4. Release instants and interval and three ETC strategies.

REFERENCES

[1] B. V. Solanki, A. Raghurajan, K. Bhattacharya and C. A. Cañizares, "Including Smart Loads for Optimal Demand Response in Integrated Energy Management Systems for Isolated Microgrids," *IEEE Trans. Smart Grid*, vol. 8, no. 4, pp. 1739-1748, 2017.

[2] F. Perez, G. Damm, C. M. Verrelli and P. F. Ribeiro, "Adaptive Virtual Inertia Control for Stable Microgrid Operation Including Ancillary Services Support," *IEEE Trans. Control Syst. Technol.*, vol. 31, no. 4, pp. 1552-1564, 2023.

[3] Y. Zhang, R. Zhong, and H. Yu, "Mitigating stop-and-go traffic congestion with operator learning," *Transp. Res. Part C Emerg. Technol.*, vol. 170, no. 104928, 2025.

[4] Y. Zhang, H. Yu, J. Auriol, and M. Pereira, "Mean-square exponential stabilization of mixed-autonomy traffic PDE system," *Automatica*, vol. 170, no. 111859, 2024.

[5] X. Ge, D. G. Lui, C. Motta, A. Petrillo, and S. Santini, "SOTIF-Oriented Distributed Control for Connected Autonomous Vehicles Platoons," *IEEE Trans. Syst., Man, Cybern.: Syst.*, 2025.

[6] S. Zhang, Z. W. Liu, Y. Zhai, Y. Zhao, and G. Wen, "Constant-stepsize distributed optimization algorithm with malicious nodes," *2021 Int. Conf. Neuromorphic Comput.*, pp. 177-182, 2021.

[7] L. Wang, X. Wang, and Z. Wang, "Event-triggered optimal tracking control for strict-feedback nonlinear systems with non-affine nonlinear faults," *Nonlinear Dyn.*, vol. 112, no. 17, pp. 15413-15426, 2024.

[8] S. Zhang, Z. Liu, G. Wen, and Y. Wang, "Accelerated distributed optimization algorithm with malicious nodes," *IEEE Trans. Netw. Sci. Eng.*, vol. 11, no. 2, pp. 2238–2248, 2023.

[9] L. Xu, X. Yi, Y. Shi, K.H. Johansson, T. Chai and T. Yang, "Distributed nonconvex optimization with event-triggered communication," *IEEE Trans. Autom. Control.*, vol. 69, no. 4, pp. 2745–2752, 2023.

[10] P. Tabuada, "Event-Triggered Real-Time Scheduling of Stabilizing Control Tasks," *IEEE Trans. Autom. Control.*, vol. 52, no. 9, pp. 1680-1685, 2007.

[11] A. Anta and P. Tabuada, "To Sample or not to Sample: Self-Triggered Control for Nonlinear Systems," *IEEE Trans. Autom. Control.*, vol. 55, no. 9, pp. 2030-2042, 2010.

[12] K. J. Åström and B. Bernhardsson, "Comparison of periodic and event based sampling for first-order stochastic systems," *IFAC Proceedings Volumes*, vol. 32, no. 2, pp. 5006-5011, Jul. 1999.

[13] D. Theodosis and D. V. Dimarogonas, "Event-Triggered Control of Nonlinear Systems With Updating Threshold," *IEEE Control Syst. Lett.*, vol. 3, no. 3, pp. 655-660, 2019.

[14] P. Elena, P. Romain, A. Daniele, N. Dragan and H. W. Maurice, "Decentralized event-triggered estimation of nonlinear systems,"*Automatica*, vol. 160, pp. 111414, 2024.

[15] Z. M. Wang, "Hybrid Event-triggered Control of Nonlinear System with Full State Constraints and Disturbance," *36th Chinese Control Decis. Conf.*, pp. 2122-2127, 2024.

[16] R. Postoyan, A. Anta, W. P. M. H. Heemels, P. Tabuada and D. Nešić, "Periodic event-triggered control for nonlinear systems," *52nd IEEE Conf. Decis. Control*, pp. 7397-7402, 2013.

[17] N. Pang, L. Y. Huang, B. T. Dong, H. T. Chen, Z. H. Jia and W. D. Zhang, "Safe Policy Optimization With Stretchable Penalties," *Authorea Preprints*, DOI:10.36227/techrxiv.173092241.15952706/v1 2024.

[18] L. T. Xing, C. Y. Wen, Z. T. Liu, H. Y. Su, and J. P. Cai, "Event-Triggered Adaptive Control for a Class of Uncertain Nonlinear Systems," *IEEE Trans. Auto. Cont.*, vol. 62, no. 4, pp. 2071-2076, 2017.

[19] G. Jiang, Y. Wang, Y. Li, N. S. Moosavi, and P. Hui, "Blending social interaction realms: Harmonizing online and offline interactions through augmented reality," in *17th Int. Symp. Visual Inf. Commun. Interact.*, pp. 1–8, 2024.

[20] K. Zhou, Z, Wang, Z. Chen, and X. Wang, "Event-Triggered Observer-Based Fixed-Time Consensus Control for Uncertain Nonlinear Multiagent Systems with Unknown States," *the 3rd Int. Conf. Neuromorphic Comput.*, early accepted, 2024. Available: arXiv:2501.00523.

[21] C. L. P. Chen, G. X. Wen, Y. J. Liu, and Z. Liu, "Observer-based adaptive backstepping consensus tracking control for high-Order nonlinear semi-strict-feedback multiagent systems,"*IEEE Trans. Cybern.*, vol. 46, no. 7, pp. 1591–1601, 2016.

[22] Z. M. Wang, X. Wang and N. Pang, "Adaptive Fixed-Time Control for Full State-Constrained Nonlinear Systems: Switched-Self-Triggered Case" *IEEE Trans. Circuits Syst. II Express Briefs*, vol. 71, no. 2, pp. 752–756, 2024.

[23] N. Pang, X. Wang and Z. M. Wang, "Observer-Based Event-Triggered Adaptive Control for Nonlinear Multiagent Systems With Unknown States and Disturbances," *IEEE Trans. Neural Netw. Learn. Syst.*, vol. 34, no. 9, pp. 6663-6669, Sept. 2023.

[24] S. J. Yoo, "Distributed consensus tracking for multiple uncertain nonlinear strict-feedback systems under a directed graph," *IEEE Trans. Neural Netw. Learn. Syst.*, vol. 24, no. 4, pp. 666–672, 2013.

[25] L. Liu and X. Li, "Event-Triggered Tracking Control for Active Seat Suspension Systems With Time-Varying Full-State Constraints," *IEEE Trans. on Syst. Man Cybern. Syst.*, vol. 52, no. 1, pp. 582-590, 2022.

[26] Z. M. Wang, H. Wang, X. Wang, N. Pang and Q. Shi, "Event-Triggered Adaptive Neural Control for Full State-Constrained Nonlinear Systems with Unknown Disturbances" *Cogn. Comput.*, vol. 16, no. 2, pp. 717–726, 2023.

[27] T. Henningsson, E. Johannesson, and A. Cervin, "Sporadic event-based control of first-order linear stochastic systems,"*Automatica*, vol. 44, no. 11, pp. 2890–2895, 2008.

[28] N. Pang, X. Wang, and Z. Wang, "Event-triggered adaptive control of nonlinear systems with dynamic uncertainties: The switching threshold case," *IEEE Trans. Circuits Syst. II Express Briefs*, vol. 69, no. 8, pp. 3540-3544, 2022.

[29] G. Zhang, X. Wang, Z. Wang, and N. Pang, "Optimized backstepping tracking control using reinforcement learning for strict-feedback nonlinear systems with monotone tube performance boundaries," *Int. J. Control*, pp. 1–13, 2025.